EurJIC European Journal of Inorganic Chemistry

FULL PAPER

DOI: 10.1002/ejic.201200733

Arene–Ruthenium Complexes with Phosphanylferrocenecarboxamides Bearing Polar Hydroxyalkyl Groups – Synthesis, Molecular Structure, and Catalytic Use in Redox Isomerizations of Allylic Alcohols to Carbonyl Compounds

Jiří Schulz,[a] Ivana Císařová,[a] and Petr Štěpnička*[a]

Dedicated to the memory of Professor Jaroslav Podlaha

Keywords: Metallocenes / Structure elucidation / Isomerization / Phosphane ligands / Ruthenium

Phosphanylferrocenecarboxamide Ph_2P–fc–$CONHCH_2$-CH_2OH (**1**, fc = ferrocene-1,1′-diyl) and its newly synthesized congeners, Ph_2P–fc–$CONHCH(CH_2OH)_2$ (**2**) and Ph_2P–fc–$CONHC(CH_2OH)_3$ (**3**), were converted to a series of (η^6-arene)ruthenium complexes [(η^6-arene)$RuCl_2$(L-κ*P*)] **5**–**7**, where arene is benzene, *p*-cymene, and hexamethylbenzene and L = **1**–**3**. All compounds were characterized by multinuclear NMR and IR spectroscopy, by mass spectrometry, and by elemental analysis,. The molecular structures of **2**, **3**, **3O** (a phosphane oxide resulting from the oxidation of **3**), **5c**·CH_2Cl_2, and **6c**·Et_2O were determined by single-crystal X-ray diffraction analysis. The ruthenium complexes were further evaluated as catalysts in the redox isomerization of allyl alcohols to carbonyl compounds. Complex [(η^6-*p*-cymene)$RuCl_2$(**1**-κ*P*)] (**5b**) proved to be a particularly attractive catalyst, being both readily available and catalytically active. Substrates with unsubstituted double bonds were cleanly isomerized with this catalyst in 1,2-dichloroethane (0.5 mol-% Ru, 80 °C), whereas for those bearing substituents at the double bond (particularly in the position closer to the OH group) lower conversions and selectivities were achieved. A similar trend was noted when pure water was used as the solvent, except that the best results (complete conversion with 2 mol-% Ru) were seen for 1,3-diphenylallyl alcohol, the most hydrophobic substrate.

Introduction

Phosphanyl-carboxamides are versatile ligands, having manifold applications in catalysis.[1] The possibility of a practically unlimited combination of various molecular fragments achieved by amide coupling makes phosphanyl-carboxylic amides structurally very flexible and can be advantageously utilized in the preparation of purpose-tailored donors. In such compounds, the phosphanyl moiety typically acts as a metal binding site, whereas the amide moiety is used to impart the desired property, to increase the affinity of these donors and their complexes toward a particular solvent or phase, or to do both. For instance, a number of ligands have been designed by using this approach, which were used in transition-metal-catalyzed reactions performed in ionic liquids, water, and mixed-solvent aqueous reaction media.[1,2]

Rather surprisingly, only a handful of such modified donors have been reported for the practically very successful phosphanylferrocene ligands.[3,4] Pugin et al. prepared chiral phosphanylferrocene donors (Josiphos analogues) bearing polar, solvent-directing imidazolium and polycarboxylate tags.[5] We have recently reported several polar ferrocene-based amidophosphane donors prepared by the conjugation of 1′-(diphenylphosphanyl)ferrocene-1-carboxylic acid (Hdpf; Scheme 1)[6] with aminosulfonic acids,[7] amino acids,[8] or hydroxyalkyl-substituted amines.[9] Since phosphanylamides bearing hydroxyalkyl substituents have only few precedents, even among simple (organic) ligands,[10–12] we set out to extend our earlier study focused on ligand **1**[9,13] (Scheme 1) toward the structurally related bis- and tris(hydroxymethyl)methanamine derivatives **2** and **3**.

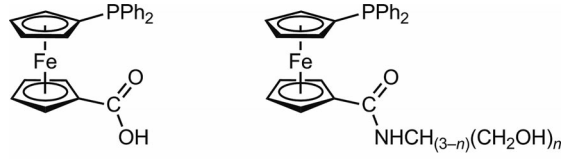

Hdpf **1** (*n* = 1), **2** (*n* = 2), **3** (*n* = 3)

Scheme 1.

[a] Department of Inorganic Chemistry, Faculty of Science, Charles University in Prague,
Hlavova 2030, 12840 Prague, Czech Republic
Fax: +420-221-951-253
E-mail: stepnic@natur.cuni.cz
Homepage: http://web.natur.cuni.cz/~stepnic/

Supporting information for this article is available on the WWW under http://dx.doi.org/10.1002/ejic.201200733.

This work describes the preparation and structural characterization of the new phosphanylferrocene hydroxyalkyl-substituted amides **2** and **3** and of (η^6-arene)ruthenium complexes featuring compounds **1**–**3** as P-monodentate ligands. Also reported are the results of catalytic tests of the Ru complexes in the redox isomerization of allylic alcohols to carbonyl compounds.

Results and Discussion

Synthesis and Structural Characterization of the Ligands

The (2-hydroxyethyl)-substituted amide **1** was obtained by the amide coupling of Hdpf with (2-hydroxyethyl)amine upon the action of 1-ethyl-3-[(3-dimethylamino)propyl]-carbodiimide and 1-hydroxybenzotriazole as reported earlier.[9a] Amides **2** and **3**, completing the series of structurally related ligands, have been prepared similarly (Scheme 2) by the direct reaction of Hdpf with an excess of the respective amine in the presence of 2-ethoxy-1-(ethoxycarbonyl)-1,2-dihydroquinoline (EEDQ) as an amide coupling agent and 4-(dimethylamino)pyridine (DMAP) as a base in pyridine solvent. The coupling agent was chosen mainly to avoid an undesired formation of esters.[14,15] This procedure afforded amides **2** and **3** in good yields (40 and 56%, respectively) after isolation by column chromatography and subsequent crystallization from ethyl acetate/hexane. Alternatively, compound **3** was synthesized from the active pentafluorophenyl ester **4**[9a,16] and 2-amino-2-(hydroxymethyl)propane-1,3-diol (TRIS; route B in Scheme 2). However, this reaction performed in the presence of DMAP in DMF at room temperature afforded the amide with a considerably lower isolated yield (27%).

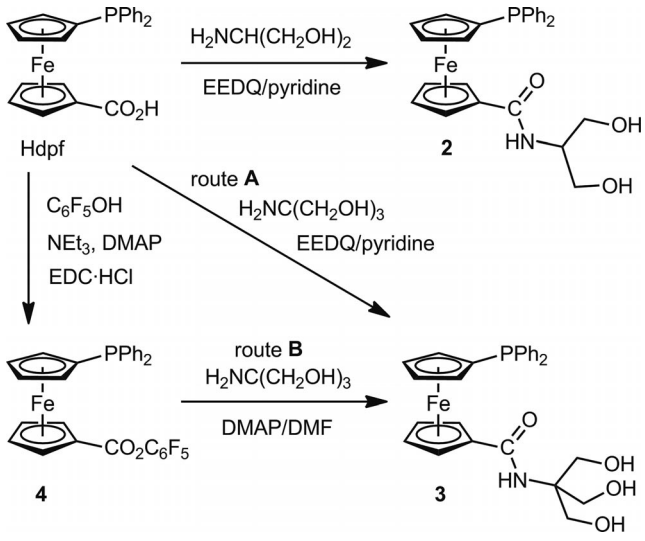

Scheme 2. Synthesis of amides **2** and **3**. Legend: EEDQ = 2-ethoxy-1-(ethoxycarbonyl)-1,2-dihydroquinoline, EDC = 1-[3-(dimethylamino)propyl]-3-ethylcarbodiimide, DMF = *N*,*N*-dimethylformamide, DMAP = 4-(dimethylamino)pyridine.

The formulations of amides **2** and **3** were confirmed by elemental analyses and by electrospray ionization (ESI) mass spectra that show abundant pseudomolecular ions ([M – H]$^-$). The NMR spectra of **2** and **3** comprise signals of the 1′-(diphenylphosphanyl)ferrocen-1-yl group and the amide pendants. It is noteworthy that the positions of the ^{1}H, ^{13}C{^{1}H}, and ^{31}P{^{1}H} NMR signals of the former moiety are practically identical with those found for **1**. Differences are seen for the signals of the $NHCH_{3-n}(CH_2OH)_n$ groups, which shift to the lower field in both ^{1}H and ^{13}C{^{1}H} NMR spectra upon increasing the substitution at the α-C atom (i.e., with increasing *n*). The presence of the amide moiety is clearly manifested in the IR spectra through characteristic amide I (ca. 1620 cm^{-1}), amide II (ca. 1540 cm^{-1}), and ν_{NH} bands (3260–3300 cm^{-1}).

Molecular Structures of Compounds 2, 3, and 3O

Single crystals of **2** and **3** suitable for X-ray diffraction analysis were grown from ethyl acetate/hexane. The same procedure also afforded crystals of phosphane oxide **3O**, a compound resulting from the slow oxidation of the parent phosphane **3** with air. This compound was prepared intentionally by the reaction of **3** with hydrogen peroxide (see Exp. Sect.). Views of the molecular structures of **2**, **3**, and **3O** are presented in Figures 1, 2, and 3, respectively. Selected geometric data are summarized in Table 1.

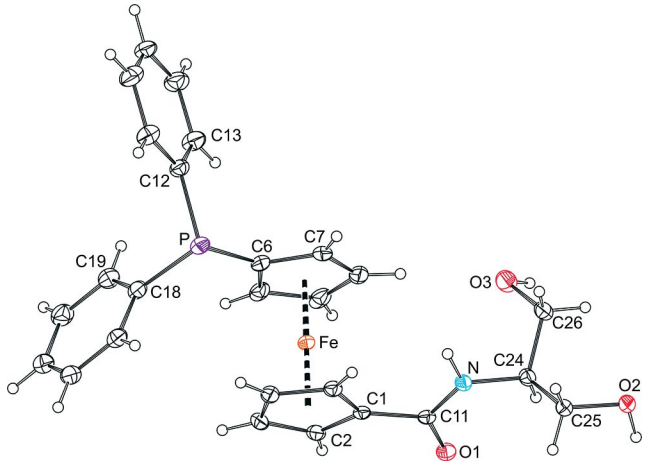

Figure 1. PLATON plot of the molecular structure of compound **2** showing the atom labeling scheme and displacement ellipsoids at the 30% probability level.

The ferrocene moieties in **2**, **3**, and **3O** are regular, showing marginal variations in the individual Fe–C distances and, accordingly, tilt angles of only approximately 1°. The structures differ by the orientation of the substituents attached to the ferrocene moiety. As indicated by the torsion angles τ in Table 1, the cyclopentadienyl rings in **2** and **3** adopt a conformation close to anticlinal eclipsed (ideal value: τ = 144°) and synclinal eclipsed (ideal value: τ = 72°), respectively, whereas in **3O** they assume an intermediate orientation. In all three cases, the amide substituents are rotated out of the plane of their bonding cyclopentadienyl ring Cp1. The largest deviation from a coplanar arrangement is seen for compound **3** (see ϕ angle in Table 1). Other-

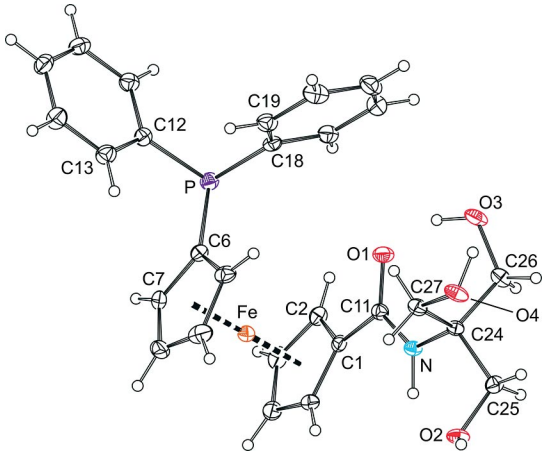

Figure 2. PLATON plot of the molecular structure of compound **3**. Displacement ellipsoids are drawn at the 30% probability level.

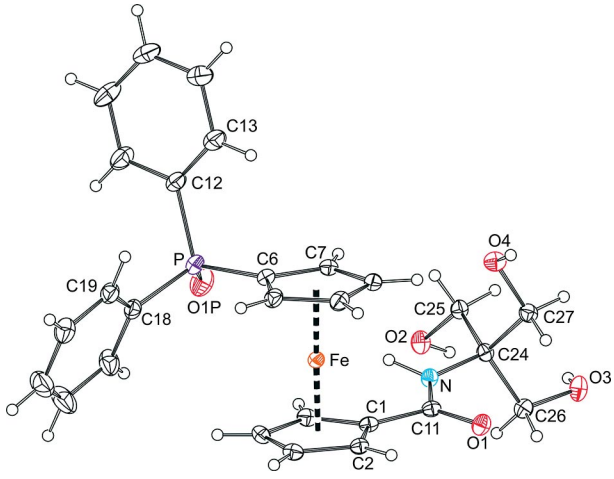

Figure 3. PLATON plot of the molecular structure of phosphane oxide **3O**. Displacement ellipsoids are drawn at the 30% probability level.

Table 1. Selected geometric data for **2**, **3**, and **3O** [distances in Å and angles in °].

Parameter[a]	**2**	**3**	**3O**[b]
Fe–C	2.037(2)–	2.022(3)–	2.032(2)–
(range)	2.053(3)	2.047(3)	2.071(2)
Fe–Cg1	1.651(1)	1.641(1)	1.6597(9)
Fe–Cg2	1.643(1)	1.639(1)	1.658(1)
tilt	1.0(1)	1.3(2)	0.9(1)
τ	152.4(2)	79.2(2)	121.4(1)
C1–C11	1.477(3)	1.478(3)	1.482(3)
C11–O1	1.239(2)	1.242(3)	1.236(2)
C11–N	1.347(2)	1.344(3)	1.346(3)
O1–C11–N	122.3(2)	123.8(2)	123.4(2)
ϕ	17.8(2)	24.7(3)	11.1(2)
C6–P	1.805(3)	1.821(3)	1.775(2)

[a] Definition of the ring planes: Cp1 = C(1–5), Cp2 = C(6–10); Cg1 and Cg2 are the centroids of the rings Cp1 and Cp2. Tilt = dihedral angle subtended by planes Cp1 and Cp2; τ = torsion angle C1–Cg1–Cg2–C6. ϕ is the dihedral angle of planes Cp1 and {C11,N,O1}. [b] Further data: P–O1P 1.456(2) Å.

wise, the molecular structures compare well with those determined for other uncoordinated Hdpf-based amides.[7,8a,9a,17]

In their crystals, compounds **2**, **3**, and **3O** form complicated supramolecular arrays through hydrogen-bonding interactions of their polar amide pendants. In the case of **2**, the individual molecules combine into centrosymmetric pairs by forming O2–H2O···O1 hydrogen bonds (Figure 4, a; for parameters, see Table 2). These dimers, stabilized by intramolecular C8–H8···O3 contacts, are connected to proximal molecules by means of N–H1N···O2 and C2–H2···O3 interactions to form layers oriented parallel to the *bc* plane (Figure 4, b). The assembly is further stabilized by O3–H3O···P contacts (Figure 4, c) directed above and below the mentioned dimeric units (the O3 atom acts already as an acceptor for two C–H bonds). This rather peculiar interaction is manifested by a distinct electron density peak

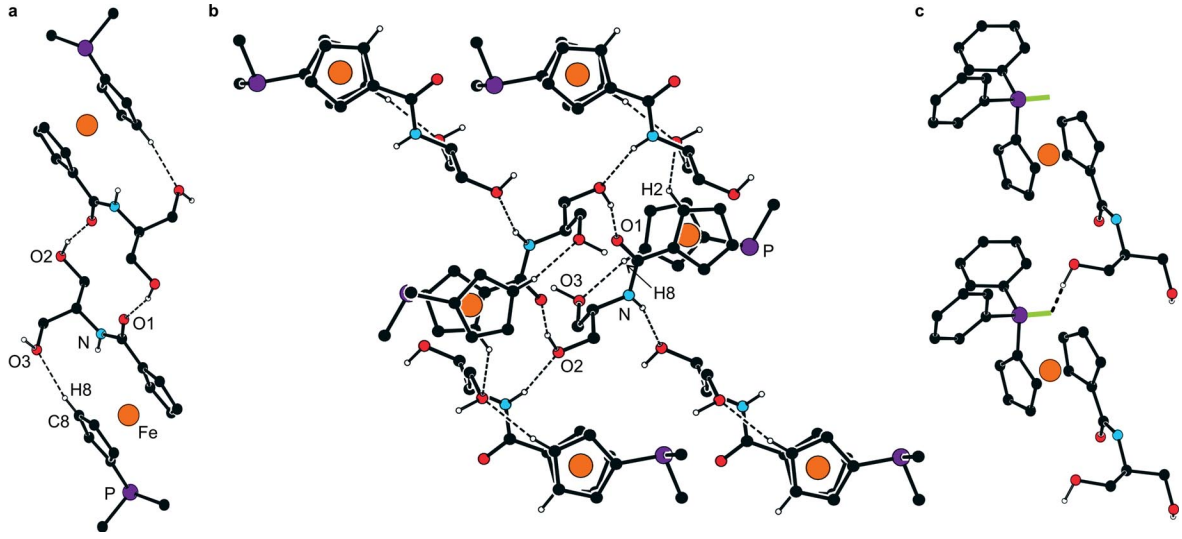

Figure 4. Packing diagrams for compound **2**. (a) View of the hydrogen-bonded dimeric motif in the structure of **2**; (b) full view showing the same dimeric unit and its interactions with adjacent molecules; (c) O–H···P contacts between molecules related by elemental translation along the *y* axis. For clarity, only OH and NH hydrogen atoms and pivotal carbon atoms from the phenyl rings (in parts a and b) are shown. The hydrogen bonds are indicated with dashed lines (for parameters, see Table 2). In part c, the green lines connect the phosphorus atoms with the refined electron density maxima (see Exp. Sect.).

in an appropriate position, which corresponds to the lone electron pair at the phosphorus (see Exp. Sect.). Although considerably weaker than the conventional O···H–O and O···H–N hydrogen bonds operating in the structure of **2**, the P···H–O interactions have been documented by spectroscopic measurements[18] and can be detected in the crystal structures of other hydroxyphosphanes (including ferrocene-based ones[19]) and adducts formed from phosphanes and alcohols.[20] It is also noteworthy that the basic dimeric motif in **2** as well as its interactions with adjacent molecules are the *same* as those found in the structure of **1**, from which **2** actually differs by the added CH_2OH arm, which enters into the O–H···P interactions with molecules located above and below the dimeric unit.

Table 2. Hydrogen bond parameters for **2**, **3**, and **3O**.[a]

D–H···A[b]	D···A distance [Å]	D–H···A angle [°]
Compound **2**		
N–H1N···O2^{i}	3.103(2)	163
O2–H2O···O1^{ii}	2.745(2)	163
O3–H3O···P^{iii}	3.282(2)	155
C2–H2···O3^{iv}	3.126(3)	132
C8–H8···O3 (*I*)	3.317(3)	166
Compound **3**		
N–H1N···O2 (*I*)	2.778(3)	107
N–H1N···O2^{v}	2.952(3)	157
O2–H2O···O4^{vi}	2.675(2)	168
O3–H3O···O1 (*I*)	2.582(3)	152
O4–H4O···O3^{vii}	2.679(2)	165
Compound **3O**		
N–H1N···O2^{viii}	3.236(2)	170
O2–H2O···O1P^{viii}	2.755(2)	163
O3–H3O···O1P^{viii}	2.695(2)	161
O4–H4O···O1^{ix}	2.780(2)	157
C3–H3···O4^{x}	3.254(2)	153
C5–H5···O2^{viii}	3.288(2)	142
C8–H8···O1^{ix}	3.444(3)	169
C9–H9···O3^{ix}	3.465(3)	157

[a] D = donor, A = acceptor. [b] Symmetry operations, *i*: 1 – *x*, *y* – 1/2, 3/2 – *z*; *ii*: 1 – *x*, 2 – *y*, 1 – *z*; *iii*: *x*, *y* + 1, *z*; *iv*: *x*, 3/2 – *y*, *z* – 1/2; *v*: 1 – *x*, –1 – *y*, –*z*; *vi*: 2 – *x*, –1 – *y*, –*z*; *vii*: 2 – *x*, –*y*, –*z*, *viii*: 2 – *x*, –*y*, 1 – *z*; *ix*: 2 – *x*, –*y*, 2 – *z*; *x*: *x* – 1, *y*, *z*. (I) denotes an intramolecular contact.

The crystal packing of **3** is also dominated by hydrogen-bonding interactions of the amide moieties but lacks supportive C–H···O contacts (Figure 5). Each amide unit of **3** forms a closed array with its inversion-related counterpart, where the H1N and O2 atoms act as bifurcated hydrogen-bond donors and acceptors, respectively.[21] Combined with additional inter- and intramolecular hydrogen bonds formed by the remaining OH groups, the O–H···O and N–H···O interactions give rise to sheets oriented along the *ab* plane. The bulky (phosphanyl)ferrocenyl moieties extend above and below these sheets and thus encase these polar sheets.[22]

As expected, the polarized P=O group[23] in **3O** takes part in hydrogen bonding (Figure 6). The individual molecules assemble into pairs around an inversion centers through N–H···OH and O–H···O=P hydrogen bonds. These

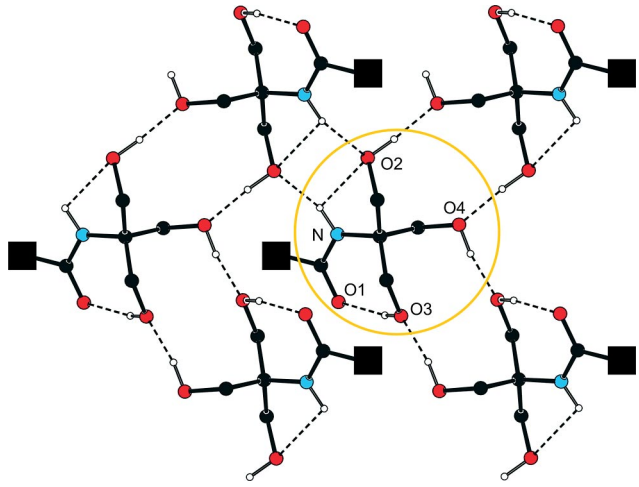

Figure 5. Section of a hydrogen-bonded array in the structure of **3**. For clarity, only the OH and NH hydrogens are shown and the bulky (phosphanyl)ferrocenyl moieties were replaced with black squares.

dimers are further connected to adjacent dimer units by O–H···O=C interactions, forming double stranded ribbons oriented along the *c* axis. Some C–H···O contacts (Table 2) operate synergistically with these conventional hydrogen bonds.

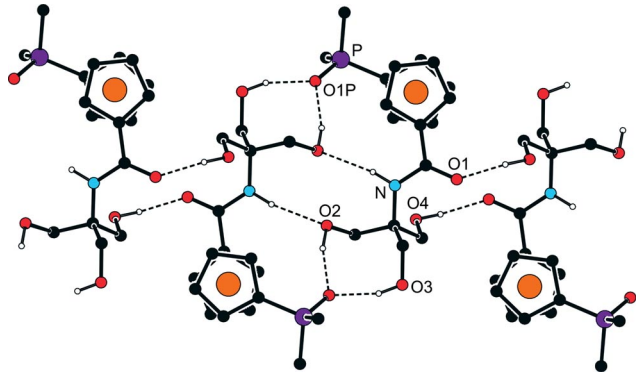

Figure 6. Hydrogen-bonded ribbons in the structure of **3O**. Only OH and NH hydrogen atoms and pivotal carbon atoms from the phenyl rings are shown for clarity.

Synthesis and Structural Characterization of (η^6-Arene)Ru^{II} Complexes

Ligands **1**–**3** were employed in the preparation of the (η^6-arene)Ru^{II} complexes **5**–**7** (Scheme 3). These complexes

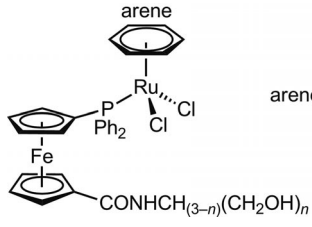

Ligand (n)	1	2	3
benzene	**5a**	**6a**	**7a**
arene = *p*-cymene	**5b**	**6b**	**7b**
C_6Me_6	**5c**	**6c**	**7c**

Scheme 3.

were readily synthesized through bridge-cleaving reactions of the respective chloride dimers $[(\eta^6\text{-arene})RuCl_2]_2$ with stoichiometric amounts of the corresponding phosphanylferrocene ligands and were purified by column chromatography.

The coordination of the ligands **1**–**3** to the (C_6H_6)Ru and (*p*-cymene)Ru fragments results in a characteristic shift of one ^{1}H NMR signal assigned to ferrocene-CH protons to a higher field (δ_H = 3.17–3.72 ppm). In the case of (C_6Me_6)Ru complexes, this signal is not observed because of extensive broadening, which probably reflects a hindered molecular mobility resulting from spatial interactions of the bulky Ru-bound arene and the (phosphanyl)ferrocenyl moiety. Similar features have been observed in the spectra of $[(\eta^6\text{-arene})RuCl_2(L)]$ complexes with other phosphanylferrocenecarboxamides (L).[8d] The $^{31}P\{^1H\}$ NMR spectra of **5**–**7** comprise singlet resonances at δ_P = 16–20 ppm,[24] whereas the ESI MS spectra of **5**–**7** are dominated by ions resulting from a simultaneous elimination of Cl^- and HCl, $[M - Cl - HCl]^+$.

The molecular structures of the solvates **5c**·CH_2Cl_2 and **6c**·Et_2O were determined by single-crystal X-ray diffraction analysis (Figures 7 and 8; Table 3). Both compounds possess the expected three-legged piano stool structures, similar to the one earlier determined for $[(\eta^6\text{-}p\text{-cymene})RuCl_2$-(Hdpf-κ*P*)].[25] The Cl–Ru–Cl and Cl–Ru–P angles do not depart much from the 90° angle expected for a pseudo-octahedral structure, in which the arene ligand occupies one trigonal face of the octahedron. On the other hand, the Cg–Ru–Cl and Cg–Ru–P angles, involving the centroid of the benzene ring (Cg), differ significantly from each other (Cg–Ru–Cl 123–126°; Cg–Ru–P 134–135°),[26] which reflects unlike steric demands of the chloride and the phosphanylferrocene ligands. Despite this distortion, however, only a negligible slanting of the piano-stool structure is seen, as indicated by the dihedral angle of the basal plane {Cl1,Cl2,P} and the η^6-arene ring being 4.33(8)° and 5.8(1)° for **5c**·CH_2Cl_2 and **6c**·Et_2O, respectively. The planes of the Ru-bound arene ring and the phosphanyl-substituted cyclopentadienyl ring (Cp2) are mutually rotated by approximately 20°.[27] The ferrocene cyclopentadienyl rings are tilted by approximately 6° and their substituents adopt an anticlinal eclipsed conformation (cf. the ideal value: τ = 144°). Like the free ligands, the complexes form hydrogen-bonded supramolecular assemblies in the solid state. Diagrams depicting the crystal packing of **5c**·CH_2Cl_2 and **6c**·Et_2O are presented in the Supporting Information (Figures S1 and S2).

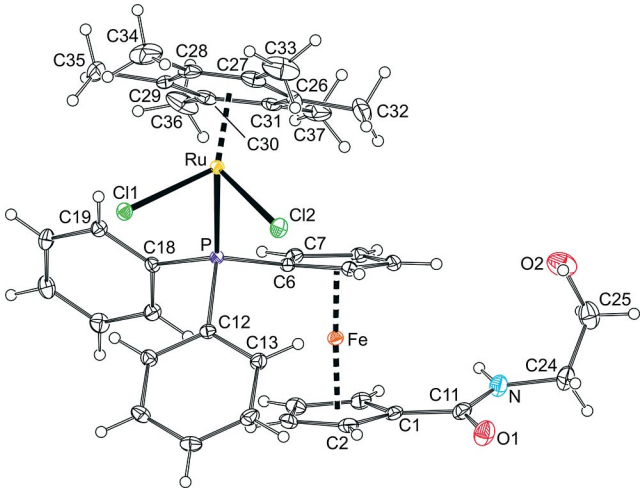

Figure 7. PLATON plot of the complex molecule in the structure of **5c**·CH_2Cl_2. Displacement ellipsoids are drawn at the 30% probability level.

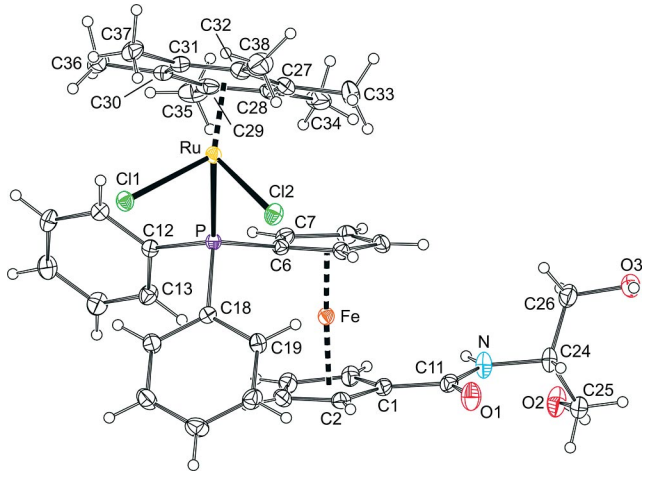

Figure 8. PLATON plot of the complex molecule in the structure of **6c**·Et_2O. Displacement ellipsoids are drawn at the 30% probability level.

Table 3. Selected geometric data for **5c**·CH_2Cl_2 and **6c**·Et_2O [distances in Å and angles in °].

Parameter[a]	**5c**·CH_2Cl_2	**6c**·Et_2O
Ru–Cl1	2.4232(6)	2.4132(6)
Ru–Cl2	2.4228(6)	2.4141(7)
Ru–P	2.3443(5)	2.3569(6)
Ru–C (range)	2.202(2)–2.271(3)	2.211(3)–2.252(3)
Cl1–Ru–Cl2	88.13(2)	88.13(2)
Cl1–Ru–P	85.29(2)	83.59(2)
Cl2–Ru–P	85.99(2)	85.76(2)
Fe–Cg1	1.651(1)	1.650(1)
Fe–Cg2	1.654(1)	1.649(1)
tilt	6.1(1)	5.6(2)
τ	143.0(2)	141.9(2)
C11–O1	1.236(3)	1.239(3)
C11–N	1.344(3)	1.335(3)
O1–C11–N	121.7(2)	121.3(3)
ϕ	13.7(3)	4.9(3)

[a] Definition of the ring planes: Cp1 = C(1–5), Cp2 = C(6–10); Cg1 and Cg2 are the centroids of the rings Cp1 and Cp2. Tilt: dihedral angle subtended by the planes Cp1 and Cp2; τ is the torsion angle C1–Cg1–Cg2–C6. ϕ denotes the dihedral angle of the planes Cp1 and {C11,N,O1}.

Catalytic Tests

The transition-metal-catalyzed isomerization of allylic alcohols to saturated carbonyl compounds represents a synthetically useful, atom-economical process, the importance

of which has been growing over the last decade.[28] In recent years, the main effort was focused on the development of efficient catalytic systems that promote this reaction under mild conditions and in short reaction times.[29,30] The progress achieved in turn allowed for the development of various tandem processes (e.g., isomerization and C–C coupling or isomerization and C–F bond formation)[29b] and even an asymmetric variant of this reaction.[31,32] Water as a green solvent with specific properties[33] and has been used advantageously as a medium for this reaction has often been employed together with Ru^{II} and Ru^{IV} catalysts.[34] Recent applications of arene–ruthenium(II) complexes of the type [(η^6-arene)$RuCl_2$(L)], where L stands for a hydrophilic ligand,[35] prompted us to test our ruthenium complexes **5**–**7** as defined catalyst precursors for this reaction.

The complexes were firstly assessed in the redox isomerization of the model substrate 1-octen-3-ol (Scheme 4) by using 0.5 mol-% of the metal catalyst and 2.5 mol-% of KO*t*Bu as a base. Complex **5b**, obtained from the most easily accessible Ru precursor and the simplest ligand, was chosen for the initial catalytic tests aimed at an optimization of the reaction conditions.

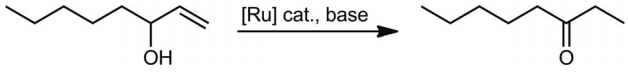

Scheme 4. The model redox isomerization of 1-octen-3-ol to octan-3-one.

Gratifyingly, the model isomerization reaction selectively produced octan-3-one with complete conversion within 1 h in both 1,2-dichloroethane and dioxane at 80 °C. A similar reaction in *N*-methylpyrrolidone afforded the ketone with 33% conversion, whereas reactions performed in *N*,*N*-dimethylformamide, *N*,*N*-dimethylacetamide, dimethyl sulfoxide, propionitrile, and 1-propanol did not proceed in any appreciable extent. The reaction in pure water afforded the desired product with 55% conversion after 1 h (at 80 °C), but, surprisingly, no reaction was observed in a 1:1 water–dioxane mixture under similar conditions. The reaction in 1,2-dichloroethane did not proceed in the absence of a base. On the other hand, the addition of any common base in a catalytic amount (2.5 mol-% of KO*t*Bu, KOAc, KOH, K_2CO_3, or K_3PO_4) resulted in complete conversion within 1 h.

A possible influence of the structure of the precatalysts was investigated next. The results achieved with the complexes **5**–**7** in the model reaction (0.5 mol-% Ru, 2.5 mol-% KO*t*Bu, 1,2-dichloroethane, 80 °C, 1 h) are summarized in Table 4. The data indicate that the catalytic performance depends on both the Ru-bound arene and the phosphane ligand. Complexes prepared from the ligands **1** and **2** afforded the product with practically quantitative conversions, whereas those prepared from **3** performed considerably worse. The influence of the Ru-bound arene was less pronounced. The best results were achieved with *p*-cymene complexes, whereas complexes bearing C_6Me_6, the most bulky and electron-rich arene ligand, achieved the lowest conversions. Nonetheless, all compounds **5**–**7** performed better than the related complex obtained from the parent carboxyphosphane, [(η^6-*p*-cymene)$RuCl_2$(Hdpf-κ*P*)],[25] which gave only 23% conversion under identical conditions (80 °C, 1 h).

Table 4. Results of catalytic tests, achieved with the (η^6-arene)Ru^{II} complexes **5**–**7** in the model isomerization reaction of 1-octen-3-ol to octan-3-one performed at 80 °C in 1,2-dichloroethane.[a]

Ligand/arene	Catalyst/yield[b] [%]		
	C_6H_6	*p*-Cymene	C_6Me_6
1	**5a**/100	**5b**/100	**5c**/>98
2	**6a**/100	**6b**/>98	**6c**/37
3	**7a**/29	**7b**/55	**7c**/27

[a] Substrate (1.0 mmol), catalyst (0.5 mol-%), KO*t*Bu (2.5 mol-%), 1,2-dichloroethane (4 mL), 1 h at 80 °C. [b] Determined by ^1H NMR spectroscopy. The results are an average of two independent runs.

When the catalyst loading was decreased to 0.25 mol-% (at 80 °C; see Supporting Information, Table S1), the conversions in the model isomerization reaction decreased considerably. The best results were obtained with complexes bearing the η^6-benzene ligand (**5a**: 38%, **6a**: 49%, and **7a**: 25%). Conversions achieved with all other complexes ranged from 10 to 19%. Finally, a reaction carried out at 50 °C with 0.5 mol-% **5b** showed no conversion after 1 h.

Because the course of the redox isomerization is affected by the structure of the substrate,[28,29] the readily accessible yet active catalyst **5b** (1 or 2 mol-%) was evaluated in reactions of various substituted allylic alcohols (Scheme 5). The results collected in Table 5 for reactions in 1,2-dichloroethane indicate that secondary allylic alcohols with unsubstituted double bonds are isomerized best (entries 1 and 5). The presence of any substitutents at the double bond (particularly in the position adjacent to the OH-substituted carbon) of both primary and secondary allylic alcohols results in relatively lower conversions and can also incite an undesired direct oxidation of the substrate to the respective α,β-unsaturated ketone (Scheme 5).

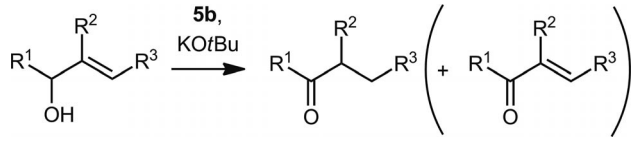

Scheme 5. Redox isomerization of substituted allylic alcohols.

When the same isomerization reactions were performed in water, surprisingly, 1,3-diphenylallyl alcohol (R^1 = R^3 = Ph, R^2 = H) was fully and cleanly converted into the corresponding saturated ketone in 20 h (**5b**: 2 mol-%). A plausible explanation could be the solubility of this compound, which is the most hydrophobic in the series and can probably form droplets, in which the catalyst accumulates (reaction "on-water").[33e,36] Among other substrates tested, only but-3-en-2-ol (R^1 = Me, R^2 = R^3 = H; 17% yield) and 2-methylprop-2-en-1-ol (R^1 = Ph, R^2 = R^3 = H, 29% yield; both are secondary alcohols with unsubstituted double bonds) were converted into the respective saturated ketones in a notable extent. Other substrates substituted at the

Table 5. Results of catalytic tests, achieved with complex **5b** in the redox isomerization of various vinyl alcohols in 1,2-dichloroethane.[a]

Entry	Substrate			Yield [%][b]			
	R^1	R^2	R^3	1 h	3 h	20 h	20 h[c]
1	Me	H	H	11 (2)	13 (3)	17 (6)	78 (3)
2	H	Me	H	0 (0)	3 (0)	4 (0)	7 (0)
3	H	H	Me	8 (0)	14 (0)	18 (7)	25 (0)
4	Me	H	Me	6 (14)	6 (20)	9 (25)	23 (37)
5	Ph	H	H	42 (0)	49 (0)	67 (0)	79 (0)
6	H	H	Ph	0 (0)	4 (5)	10 (6)	30 (6)
7	Ph	H	Ph	0 (0)	19 (0)	39 (0)	40 (0)

[a] Substrate (1.0 mmol), catalyst **5b** (1 mol-%, unless specified otherwise), and KO*t*Bu (5 mol-%) in 1,2-dichloroethane (4 mL) at 80 °C. [b] Determined by ^{1}H NMR spectroscopy. The amount of α,β-unsaturated ketone (oxidation product) is given in parentheses. [c] Reactions in the presence of 2 mol-% of the Ru catalyst.

double bond typically achieved less than 5% conversion (for the complete results, see Supporting Information, Table S2.)

Conclusions

Compounds **1**–**3** representing a complete series of structurally related phosphanylferrocenecarboxamides bearing congeneric polar hydroxyalkyl groups were utilized as P-monodentate ligands in (η^6-arene)Ru^{II} complexes of the type [(η^6-arene)$RuCl_2$(L-κ*P*)] (arene = benzene, *p*-cymene, or hexamethylbenzene; L = **1**–**3**). Both the ligands and their (η^6-arene)Ru^{II} complexes form complex supramolecular assemblies in the solid state, which are formed by means of hydrogen-bonding interactions of their polar hydroxyamide pendants. The complexes efficiently mediate the redox isomerization of allylic alcohols to the respective carbonyl compounds under moderate conditions, showing the best results for allylic alcohols with unsubstituted double bonds.

Experimental Section

Materials and Methods: All syntheses were performed under an argon atmosphere and with exclusion of the direct daylight. Hdpf,[6a] **1**,[9a] **4**,[9a,16] [(η^6-C_6H_6)$RuCl_2$]$_2$,[37] and [(η^6-C_6Me_6)-$RuCl_2$]$_2$[38] were prepared according to literature procedures. Other chemicals were obtained from commercial sources (Alfa-Aesar, Fluka, Sigma–Aldrich) and used as received. Solvents (Lachner) used for the syntheses and catalytic tests were dried with appropriate drying agents (dichloromethane, 1,2-dichloroethane, and chloroform: anhydrous potassium carbonate; 1,4-dioxane: sodium metal, acetonitrile: P_2O_5) and were freshly distilled under argon. Solvents used in crystallizations and for chromatography were used without any additional purification.

NMR spectra were recorded with a Varian Unity Inova 400 spectrometer. Chemical shifts (δ in ppm) are given relative to an internal $SiMe_4$ standard (^{1}H and ^{13}C) or an external standard of 85% aqueous H_3PO_4 (^{31}P). In addition to the standard notation of the signal multiplicity, vt and vq are used to distinguish virtual triplets and quartets, respectively, which arise from magnetically nonequivalent protons in the AA′BB′ and AA′BB′X spin systems (X = ^{31}P) of the unsymmetrically 1,1′-disubstituted ferrocene moiety (fc = ferrocene-1,1′-diyl). IR spectra were measured with an FTIR Nicolet Magna 650 spectrometer in the range 400–4000 cm^{-1}. Low-resolution electrospray ionization (ESI) mass spectra were obtained with a Bruker Esquire 3000 instrument by using methanol solutions.

1′-(Diphenylphosphanyl)-1-[*N*-(bis(hydroxymethyl)methyl)carbamoyl]ferrocene (2): Hdpf (1.66 g, 4.0 mmol), serinol (1.46 g, 16.0 mmol), 4-(dimethylamino)pyridine (24 mg, 0.2 mmol), and EEDQ (1.48 g, 6.0 mmol) were dissolved in pyridine (40 mL), and the resulting mixture was stirred first at 120 °C (temperature in the heating bath) for 1 h and then at room temperature for 1 d. The volatiles were removed under reduced pressure, and the solid residue was purified by column chromatography over silica gel. Elution with dichloromethane/methanol (50:1 v/v) led to the development of three minor bands, which were discarded. The eluent was then changed to a different dichloromethane/methanol mixture (20:1 v/v) to elute a major orange band, which was the product. After evaporation, the crude product was crystallized from a warm ethyl acetate/hexane mixture (60 mL, 1:2 v/v) by slowly cooling down to –18 °C. The resulting crystalline material was filtered off, washed with diethyl ether and pentane, and dried under vacuum; yield 0.79 g (40%), orange needles. ^{1}H NMR (400.0 MHz, $CDCl_3$, 25 °C): δ = 3.30 (br. s, 2 H, OH), 3.91 (m, 4 H, CH_2O), 4.07 (m, 1 H, NHC*H*), 4.10 (vq, J' = 1.8 Hz, 2 H, CH of fc), 4.20 (vt, J' = 2.0 Hz, 2 H, CH of fc), 4.46 (vt, J' = 1.8 Hz, 2 H, CH of fc), 4.62 (vt, J' = 2.0 Hz, 2 H, CH of fc), 6.61 (d, $^3J_{HH}$ = 7.4 Hz, 1 H, NH), 7.31–7.39 (m, 10 H, PPh_2) ppm. ^{13}C{^{1}H} NMR (100.6 MHz, $CDCl_3$, 25 °C): δ = 52.53 (NCH), 63.96 (CH_2O), 69.70 (CH of fc), 71.61 (CH of fc), 72.76 (d, J_{PC} = 4 Hz, CH of fc), 74.60 (d, J_{PC} = 13 Hz, CH of fc), 76.36 (*C*–CONH of fc), 128.37 (d, $^3J_{PC}$ = 7 Hz, CH_{meta} of PPh_2), 128.93 (CH_{para} of PPh_2), 133.41 (d, $^2J_{PC}$ = 20 Hz, CH_{ortho} of PPh_2), 137.70 (d, $^1J_{PC}$ = 6 Hz, C_{ipso} of PPh_2), 170.72 (C=O) ppm. The signal of C–P of fc was not found. ^{31}P{^{1}H} NMR (161.9 MHz, $CDCl_3$, 25 °C): δ = –17.3 (s) ppm. IR (Nujol): $\tilde{\nu}$ = 3300 (s), 1605 (s), 1549 (s), 1346 (m), 1307 (m), 1218 (w), 1192 (w), 1161 (m), 1092 (w), 1053 (s), 964 (w), 846 (w), 822 (w), 759 (w), 743 (m), 701 (m), 523 (m), 490 (m), 453 (m) cm^{-1}. ESI-MS: *m*/*z* = 486 [M – H]$^-$. $C_{26}H_{26}FeNO_3P$ (487.30): calcd. C 64.08, H 5.38, N 2.88; found C 62.95, H 5.30, N 2.67. The compound tends to incorporate diethyl ether.

1′-(Diphenylphosphanyl)-1-[*N*-(tris(hydroxymethyl)methyl)carbamoyl]ferrocene (3)

Method A: Hdpf (1.66 g, 4.0 mmol), tris(hydroxymethyl)methylamine (1.94 g, 16.0 mmol), 4-(dimethylamino)pyridine (24 mg, 0.20 mmol), and EEDQ (1.48 g, 6.0 mmol) were dissolved in pyridine (40 mL), and the reaction mixture was first stirred at 120 °C for 1 h and then at room temperature overnight. The volatiles were removed under reduced pressure, and the solid residue was purified by column chromatography (silica gel, dichloromethane/methanol, 50:1 v/v). The first minor band was discarded, and the following one was collected and the solvent evaporated to afford a crude product, which was crystallized from warm ethyl acetate/hexane (40 mL, 1:1 v/v) by slowly cooling down to –18 °C. The obtained crystalline material was isolated by suction, washed successively with diethyl ether and pentane, and dried under vacuum; yield 1.16 g (56%), orange, microcrystalline solid.

Method B: A reaction flask was charged with active ester **4** (0.58 g, 1 mmol), tris(hydroxymethyl)methylamine (0.145 g, 1.3 mmol), and 4-(dimethylamino)pyridine (6 mg, 0.05 mmol). Dry *N*,*N*-dimethylformamide (15 mL) was added, and the resulting solution was stirred for 20 h, after which the solvent was evaporated under vacuum. The solid residue was dissolved in dichloromethane (20 mL). This solution was washed twice with a 5% aqueous solution of

citric acid (10 mL), a saturated aqueous solution of $NaHCO_3$ (20 mL), and brine (20 mL), and, finally, it was dried with $MgSO_4$. The solvent was evaporated under vacuum, and the solid residue was purified by column chromatography and crystallized as described above (method A); yield 0.137 g (27%), orange, microcrystalline solid. ^1H NMR (400.0 MHz, $CDCl_3$, 25 °C): δ = 3.73 (d, $^3J_{HH}$ = 3.9 Hz, 6 H, CH_2O), 4.11 (vq, J' = 1.8 Hz, 2 H, CH of fc), 4.23 (vt, J' = 2.0 Hz, 2 H, CH of fc), 4.44 (vt, J' = 1.8 Hz, 2 H, CH of fc), 4.52 (unresolved t, 3 H, OH), 4.59 (vt, J' = 2.0 Hz, 2 H, CH of fc), 6.89 (s, 1 H, NH), 7.31–7.39 (m, 10 H, PPh_2) ppm. $^{13}C\{^1H\}$ NMR (100.6 MHz, $CDCl_3$, 25 °C): δ = 61.58 (N*C*CH_2), 63.36 (CH_2O), 69.67 (CH of fc), 71.95 (CH of fc), 72.85 (d, J_{PC} = 4 Hz, CH of fc), 74.60 (d, J_{PC} = 14 Hz, CH of fc), 76.29 (*C*–CONH of fc), 77.54 (d, $^1J_{PC}$ = 5 Hz, C–P of fc), 128.32 (d, $^3J_{PC}$ = 7 Hz, CH_{meta} of PPh_2), 128.91 (CH_{para} of PPh_2), 133.43 (d, $^2J_{PC}$ = 20 Hz, CH_{ortho} of PPh_2), 137.74 (d, $^1J_{PC}$ = 7 Hz, C_{ipso} of PPh_2), 171.70 (C=O) ppm. $^{31}P\{^1H\}$ NMR (161.9 MHz, $CDCl_3$, 25 °C): δ = –17.7 (s) ppm. IR (Nujol): $\tilde{\nu}$ = 3262 (s), 1626 (s), 1532 (s), 1351 (m), 1305 (m), 1287 (w), 1192 (w), 1160 (w), 1124 (w), 1084 (w), 1055 (m), 1027 (s), 837 (w), 821 (w), 771 (w), 746 (m), 737 (m), 696 (s), 568 (w), 520 (w), 498 (m), 484 (m), 453 (w) cm^{-1}. ESI-MS: *m*/*z* = 516 $[M - H]^-$. $C_{27}H_{28}FeNO_4P$ (517.32): calcd. C 62.68, H 5.46, N 2.71; found C 62.62, H 5.58, N 2.60.

1′-(Diphenylphosphanoyl)-1-[*N*-(tris(hydroxymethyl)methyl)carbamoyl]ferrocene (3O): Aqueous hydrogen peroxide (0.21 mL, 30%, ca. 2 mmol) was added dropwise to a solution of phosphane **3** (103.5 mg, 0.2 mmol) in acetone (15 mL) with stirring and cooling in ice. After 30 min, the reaction was quenched with a saturated aqueous solution of sodium thiosulfate (10 mL), and the volatiles were evaporated under vacuum. The aqueous residue was diluted with water and extracted with dichloromethane (2× 15 mL). The organic extracts were washed with brine (1× 30 mL), dried with magnesium sulfate, and the solvents were evaporated. The product was isolated by column chromatography (silica gel, dichloromethane/methanol, 10:1 v/v) as a yellow solid; yield 98 mg (92%). ^1H NMR (400.0 MHz, [D$_6$]DMSO, 25 °C): δ = 3.70 (d, $^3J_{HH}$ = 6.0 Hz, 6 H, CH_2O), 4.13 (vt, J' = 2.0 Hz, 2 H, CH of fc), 4.36 (vt, J' = 1.9 Hz, 2 H, CH of fc), 4.68 (vt, J' = 1.8 Hz, 2 H, CH of fc), 4.81 (vt, J' = 2.0 Hz, 2 H, CH of fc), 4.83 (unresolved t, $J \approx$ 6.0 Hz, 3 H, OH), 7.53–7.72 (m, 11 H, PPh_2 and NH) ppm. $^{13}C\{^1H\}$ NMR (100.6 MHz, [D$_6$]DMSO, 25 °C): δ = 60.58 (CH_2O), 62.62 (*C*NHCO), 69.99 (CH of fc), 70.57 (CH of fc), 72.61 (d, J_{PC} = 10 Hz, CH of fc), 72.91 (d, $^1J_{PC}$ = 115 Hz, C–P of fc), 74.32 (J_{PC} = 13 Hz, CH of fc), 79.12 (*C*–CONH of fc), 128.57 ($^2J_{PC}$ = 12 Hz, CH_{ortho} of PPh_2), 130.79 ($^3J_{PC}$ = 10 Hz, CH_{meta} of PPh_2), 131.95 ($^4J_{PC}$ = 2 Hz, CH_{para} of PPh_2), 132.76 ($^1J_{PC}$ = 107 Hz, C_{ipso} of PPh_2), 169.08 (C=O) ppm. $^{31}P\{^1H\}$ NMR (161.9 MHz, [D$_6$]-DMSO, 25 °C): δ = 29.9 (s) ppm. HRMS (ESI+): calcd. for $C_{27}H_{28}NO_5P^{56}Fe$ $[M]^+$ 533.1055; found 533.1057.

General Procedure for the Preparation of (η^6-Arene)Ru^{II} Complexes: A solution of the ligand (0.2 mmol) in dichloromethane (10 mL) was added to the solid ruthenium precursor {[(η^6-C_6Me_6)$RuCl_2$]$_2$ or [(η^6-cymene)$RuCl_2$]$_2$} or to its suspension in acetonitrile {[(η^6-C_6H_6)$RuCl_2$]$_2$ in 5 mL} (0.1 mmol). The resulting mixture was stirred in the dark for 2 h, and the solvent was then evaporated under reduced pressure. The crude product was purified by column chromatography over silica gel by using dichloromethane/methanol (50:1 or 20:1 v/v) as the eluent. A major reddish band was collected, and the solvents were evaporated to dryness. The solid residue was dissolved in a minimal amount of dichloromethane (1–3 mL), and this solution was added dropwise to diethyl ether (30 mL). The resulting precipitate was cooled to +4 °C overnight and collected by suction. The obtained material was washed successively with diethyl ether and pentane (10 mL each) and dried under vacuum.

[(η^6-C_6H_6)$RuCl_2$(1-κ*P*)] (5a): Yield 126 mg (86%), light, orange powder. ^1H NMR (400.0 MHz, $CDCl_3$, 25 °C): δ = 3.24 (br. s, 2 H, CH of fc), 3.60 (br. s, 2 H, CH_2N), 3.70 (br. s, 1 H, OH), 3.90 (br. s, 2 H, CH_2O), 4.35 (br. s, 2 H, CH of fc), 4.64–4.70 (m, 4 H, CH of fc), 5.30 (d, $^2J_{PH}$ = 0.8 Hz, 6 H, C_6H_6), 7.34–7.47 (m, 7 H, PPh_2 and NH), 7.69–7.80 (m, 4 H, PPh_2) ppm. $^{31}P\{^1H\}$ NMR (161.9 MHz, $CDCl_3$, 25 °C): δ = 16.3 (s) ppm. MS (ESI+): *m*/*z* = 636 [M – H – HCl]. $C_{31}H_{30}Cl_2FeNO_2PRu{\cdot}1.5H_2O$ (734.4): calcd. C 50.70, H 4.53, N 1.91; found C 50.74, H 4.52, N 1.94.

[(η^6-Cymene)$RuCl_2$(1-κ*P*)] (5b): Yield 131 mg (86%), ruby-red powder. ^1H NMR (400.0 MHz, $CDCl_3$, 25 °C): δ = 0.96 [d, $^3J_{HH}$ = 7.0 Hz, 6 H, CH(CH_3)$_2$], 1.85 (s, 3 H, CH_3), 2.59 [sept, $^3J_{HH}$ = 7.0 Hz, 1 H, C*H*(CH$_3$)$_2$], 3.19 (m, 2 H, CH of fc), 3.57 (virtual q, *J* = 4.7 Hz, 2 H, CH_2N), 3.84–3.86 (m, 2 H, CH_2O), 4.46–4.47 (m, 2 H, CH of fc), 4.48–4.49 (m, 2 H, CH of fc), 4.52 (vt, J' = 2.0 Hz, 2 H, CH of fc), 5.10–5.14 (m, 4 H, C_6H_4), 7.40–7.47 (m, 6 H, PPh_2), 7.51 (t, $^3J_{HH}$ = 5.1 Hz, 1 H, NH), 7.77–7.83 (m, 4 H, PPh_2) ppm. The resonance of the OH proton was not seen. $^{31}P\{^1H\}$ NMR (161.9 MHz, $CDCl_3$, 25 °C): δ = 17.7 (s) ppm. MS (ESI+): *m*/*z* = 692 $[M - Cl - HCl]^+$. $C_{35}H_{38}Cl_2FeNO_2PRu{\cdot}H_2O$ (768.9): calcd. C 54.67, H 5.06, N 1.82; found C 54.37, H 5.32, N 1.74.

[(η^6-C_6Me_6)$RuCl_2$(1-κ*P*)] (5c): Yield 129 mg (81%), orange powder. ^1H NMR (400.0 MHz, $CDCl_3$, 50 °C): δ = 1.67 (s, 18 H, C_6Me_6), 3.58 (virtual q, *J* = 4.9 Hz, 2 H, CH_2N), 3.63 (br. s, 1 H, OH), 3.85 (virtual q, *J* = 5.1 Hz, 2 H, CH_2O), 4.43 (br. s, 4 H, CH of fc), 4.51 (br. s, 2 H, CH of fc), 7.28–7.39 (m, 6 H, PPh_2), 7.42 (br. s, 1 H, NH), 7.72–7.90 (m, 4 H, PPh_2) ppm. A resonance of two protons at the ferrocen-1,1′-diyl backbone was not observed because of extensive signal broadening. $^{31}P\{^1H\}$ NMR (161.9 MHz, $CDCl_3$, 50 °C): δ = 19.3 (bs) ppm. MS (ESI+): *m*/*z* = 720 [M – Cl – HCl]$^+$. $C_{37}H_{42}Cl_2FeNO_2PRu$ (791.5): calcd. C 56.14, H 5.35, N 1.77; found C 56.02, H 5.37, N 1.67.

[(η^6-C_6H_6)$RuCl_2$(2-κ*P*)] (6a): Yield 136 mg (87%), orange powder. ^1H NMR (400.0 MHz, $CDCl_3$, 25 °C): δ = 3.62 (br. s, 2 H, OH), 3.98 (d, $^3J_{HH}$ = 4.1 Hz, 4 H, CH_2O), 4.19 (m, 1 H, C*H*NH), 4.38 (br. s, 2 H, CH of fc), 4.67 (br. s, 2 H, CH of fc), 4.71 (vt, J' = 1.8 Hz, 2 H, CH of fc), 5.30 (d, $^2J_{PH}$ = 0.7 Hz, 6 H, C_6H_6), 7.37–7.48 (m, 7 H, PPh_2 and NH), 7.67–7.81 (br. s, 4 H, PPh_2) ppm. A resonance of two protons at the ferrocen-1,1′-diyl backbone was not observed because of extensive signal broadening. $^{31}P\{^1H\}$ NMR (161.9 MHz, $CDCl_3$, 25 °C): δ = 16.5 (s) ppm. MS (ESI+): *m*/*z* = 666 $[M - H - HCl]^+$. $C_{32}H_{32}Cl_2FeNO_3PRu{\cdot}2H_2O{\cdot}0.4Et_2O$ (780.8): calcd. C 49.84, H 4.78, N 1.79; found C 49.62, H 4.60, N 1.75.

[(η^6-Cymene)$RuCl_2$(2-κ*P*)] (6b): Yield 143 mg (88%), light, orange powder. ^1H NMR (400.0 MHz, $CDCl_3$, 25 °C): δ = 0.94 [d, $^3J_{HH}$ = 7.0 Hz, 6 H, CH(CH_3)$_2$], 1.87 (s, 3 H, CH_3), 2.65 [sept, $^3J_{HH}$ = 7.0 Hz, 1 H, C*H*(CH$_3$)$_2$], 3.17 (br. s, 2 H, CH of fc), 3.64 (br. s, 2 H, OH), 3.92 (d, *J* = 4.0 Hz, 2 H, CH_2O), 4.14 (m, 1 H, C*H*NH), 4.48–4.49 (m, 4 H, CH of fc), 4.59 (vt, J' = 2.0 Hz, 2 H, CH of fc), 5.11 (br. s, 4 H, C_6H_4), 7.42–7.50 (m, 6 H, PPh_2), 7.51 (d, $^3J_{HH}$ = 7.1 Hz, 1 H, NH), 7.78–7.83 (m, 4 H, PPh_2) ppm. $^{31}P\{^1H\}$ NMR (161.9 MHz, $CDCl_3$, 25 °C): δ = 17.7 (s) ppm. MS (ESI+): *m*/*z* = 722 $[M - H - HCl]^+$. $C_{36}H_{40}Cl_2FeNO_3PRu{\cdot}H_2O$ (811.5): calcd. C 53.28, H 5.22, N 1.73; found C 53.08, H 5.24, N 1.73.

[(η^6-C_6Me_6)$RuCl_2$(2-κ*P*)] (6c): Yield 152 mg (93%), light, orange powder. ^1H NMR (400.0 MHz, $CDCl_3$, 50 °C): δ = 1.67 (d, $^4J_{PH}$ = 0.7 Hz, 18 H, C_6Me_6), 3.93 (br. s, 4 H, CH_2O), 4.06–4.13 (m, 1 H, C*H*NH), 4.39–4.56 (m, 6 H, CH of fc), 7.27–7.42 (m, 7 H, PPh_2

and NH), 7.76–7.90 (m, 4 H, PPh_2) ppm. Resonances of two protons at the ferrocen-1,1′-diyl backbone and of the hydroxy groups were not observed because of extensive signal broadening. $^{31}P\{^1H\}$ NMR ($CDCl_3$, 50 °C): δ = 19.6 (bs) ppm. MS (ESI+): *m*/*z* = 750 $[M - Cl - HCl]^+$. $C_{38}H_{44}Cl_2FeNO_3PRu$ (821.5): calcd. C 55.55, H 5.40, N 1.71; found C 55.32, H 5.26, N 1.63.

[(η⁶-C_6H_6)$RuCl_2$(3-κ*P*)] (7a): Yield 137 mg (83%), orange, microcrystalline solid. ^1H NMR (400.0 MHz, [D_6]DMSO, 25 °C): δ = 3.64 (d, $^3J_{HH}$ = 5.8 Hz, 6 H, CH_2O), 3.72 (vt, J' = 1.8 Hz, 2 H, CH of fc), 4.48 (br. s, 2 H, CH of fc), 4.51–4.55 (m, 4 H, CH of fc), 4.81 (t, $^3J_{HH}$ = 5.7 Hz, 3 H, OH), 5.40 (d, $^2J_{PH}$ = 0.7 Hz, 6 H, C_6H_6), 6.55 (s, 1 H, NH), 7.42–7.52 (m, 6 H, PPh_2), 7.70–7.77 (m, 4 H, PPh_2) ppm. $^{31}P\{^1H\}$ NMR (161.9 MHz, [D_6]DMSO, 25 °C): δ = 20.2 (s) ppm. MS (ESI+): *m*/*z* = 696 $[M - H - HCl]^+$. $C_{33}H_{34}Cl_2FeNO_4PRu{\cdot}H_2O{\cdot}0.6Et_2O$ (829.9): calcd. C 51.23, H 5.10, N 1.69; found C 51.02, H 4.84, N 1.70.

[(η⁶-Cymene)$RuCl_2$(3-κ*P*)] (7b): Yield 148 mg (90%), ruby-red, microcrystalline solid. ^1H NMR (400.0 MHz, [D_6]DMSO, 25 °C): δ = 0.83 [d, $^3J_{HH}$ = 7.0 Hz, 6 H, $CH(CH_3)_2$], 1.71 (s, 3 H, CH_3), 2.31 [sept, $^3J_{HH}$ = 7.0 Hz, 1 H, $CH(CH_3)_2$], 3.61 (d, $^3J_{HH}$ = 5.8 Hz, 6 H, CH_2O), 3.65 (vt, J' = 1.8 Hz, 2 H, CH of fc), 4.37–4.39 (m, 4 H, CH of fc), 4.50 (vq, J' = 1.7 Hz, 2 H, CH of fc), 4.81 (t, $^3J_{HH}$ = 5.7 Hz, 3 H, OH), 5.23 (d, J = 6.3 Hz, 2 H, C_6H_4), 5.32 (dd, J = 6.4, 1.2 Hz, 2 H, C_6H_4), 6.48 (s, 1 H, NH), 7.46–7.53 (m, 6 H, PPh_2), 7.79–7.86 (m, 4 H, PPh_2) ppm. $^{31}P\{^1H\}$ NMR (161.9 MHz, [D_6]DMSO, 25 °C): δ = 20.3 (s) ppm. MS (ESI+): *m*/*z* = 752 $[M - H - HCl]^+$. $C_{37}H_{42}Cl_2FeNO_4PRu$ (823.5): calcd. C 53.96, H 5.14, N 1.70; found C 53.75, H 5.21, N 1.58.

[(η⁶-C_6Me_6)$RuCl_2$(3-κ*P*)] (7c): Yield 154 mg (91%), ruby-red powder. ^1H NMR (400.0 MHz, $CDCl_3$, 50 °C): δ = 1.67 (s, 18 H, C_6Me_6), 3.83 (d, $^3J_{HH}$ = 4.8 Hz, 6 H, CH_2O), 4.02 (br. s, 3 H, OH), 4.39 (d, J' = 1.7 Hz, 2 H, CH of fc), 4.44 (br. s, 2 H, CH of fc), 4.53 (br. s, 2 H, CH of fc), 7.02 (br. s, 1 H, NH), 7.32–7.42 (m, 6 H, PPh_2), 7.77–7.91 (m, 4 H, PPh_2) ppm. The resonance of two protons at the ferrocen-1,1′-diyl backbone was not found because of an extensive signal broadening. $^{31}P\{^1H\}$ NMR (161.9 MHz, $CDCl_3$, 50 °C): δ = 20.1 (bs) ppm. MS (ESI+): *m*/*z* = 780 $[M - H - HCl]^+$. $C_{39}H_{46}Cl_2FeNO_4PRu$ (851.6): calcd. C 55.00, H 5.45, N 1.65; found C 54.66, H 5.64, N 1.61.

Catalytic Tests: A Schlenk tube was charged with the respective allylic alcohol (1.0 mmol) and ruthenium catalyst, a base (in appropriate amounts), and 1-methoxy-2-(2-methoxyethoxy)ethane (67 mg, 0.5 mmol) as an internal standard. The tube was flushed with argon and sealed. The solvent (4 mL) was added, and the resulting mixture was heated to 80 °C.

The conversions were determined by ^1H NMR spectroscopy. The identity of the products was confirmed by a comparison of the NMR spectra with the literature (octan-3-one, *trans*-cinnamaldehyde and propiophenone;[39] 1,3-diphenylpropan-1-one,[40] 2-butanone,[41] 2-pentanone,[42] 3-phenylpropanal,[43] 2-butenal,[44] and 3-buten-2-one[45]) or with spectra of authentic samples (butyraldehyde, 2-methylpropanal, and 3-penten-2-one).

X-ray Crystallography: Single crystals suitable for X-ray diffraction measurements were obtained by liquid-phase diffusion from ethyl acetate/hexane (**2**: orange plate, $0.20 \times 0.35 \times 0.45$ mm^3; **3**: orange plate, $0.03 \times 0.10 \times 0.25$ mm^3; **3O**: orange prism, $0.23 \times 0.38 \times 0.55$ mm^3), dichloromethane/hexane (**5c**·CH_2Cl_2: red plate, $0.20 \times 0.40 \times 0.50$ mm^3), or similarly from chloroform/methanol/hexane (**5c**·Et_2O: red bar, $0.08 \times 0.15 \times 0.30$ mm^3).

The diffraction data ($\pm h \pm k \pm l$, θ_{max} = 26–27.5°, data completeness ≥ 99.3%) were collected with a Nonius KappaCCD diffractometer equipped with a Cryostream Cooler (Oxford Cryosystems) at 150(2) K by using graphite monochromated Mo-K_α radiation (λ = 0.71073 Å) and were analyzed with the HKL program package.[46] The structures were solved by the direct methods (SIR97[47]) and refined to full convergence by full-matrix least-squares methods on the basis of F^2 (SHELXL97[48]). The non-hydrogen atoms were refined with anisotropic displacement parameters. Hydrogen atoms of the OH and NH groups were identified on the difference density maps and refined as riding atoms with U_{iso}(H) assigned to a multiple of 1.2U_{eq}(O/N). Other hydrogen atoms were included in their calculated positions and refined similarly. Relevant crystallographic data and refinement parameters are presented in Table S3 (Supporting Information). Particular details of the structure refinement are discussed in the following paragraph.

The solvent present in the structure of **6c**·Et_2O was severely disordered in structural voids, hence, its contribution to the overall scattering was removed by the SQUEEZE[49] routine incorporated in the PLATON program.[50] A total of 110 electrons were found in 566 Å^3 of void space per unit cell (four molecules of diethyl ether represent 136 electrons). It is also noteworthy that the largest electron density peak in the final difference density map (2.4 e·Å^{-3}) for compound **2** very likely corresponds to a lone electron pair at the phosphorus atom (the second largest electron density maximum is only ca. 0.35 e·Å^{-3}). This assumption was confirmed by a refinement of this "peak" as a helium atom (2 electrons), which led to a decrease in the *R* value to 2.96% and gave a reasonable geometry [P···He distance is 1.305(5) Å with a clear contact of He to H3O, which is located in a proximal molecule: He···O3 ≈ 2.36 Å, He···H3O–O3 ≈ 173°].

Geometric data and structural drawings were obtained with a recent version of the PLATON program. All numerical values are rounded with respect to their estimated deviations (ESDs) given in one decimal. Parameters relating to atoms in constrained positions (hydrogen atoms) are given without ESDs.

CCDC-889295 (for **2**), -889296 (for **3**), -889297 (for **3O**), -889298 (for **5c**·CH_2Cl_2) and -889299 (for **6c**·Et_2O) contain the supplementary crystallographic data for this paper. These data can be obtained free of charge from The Cambridge Crystallographic Data Centre via www.ccdc.cam.ac.uk/data_request/cif.

Supporting Information (see footnote on the first page of this article): Crystal packing diagrams for **5c**·CH_2Cl_2 (Figure S1) and **6c**·Et_2O (Figure S2), histograms showing the distribution of O···O distances and O–H···O angles in P=O···H–O hydrogen bonds (Figures S3 and S4), results of catalytic tests, achieved in the model redox isomerization reaction with 0.25 mol-% of **5**–**7** in 1,2-dichloroethane at 80 °C (Table S1), results of catalytic tests for the isomerization of various allylic alcohols with catalyst **5b** in water (Table S2), and a summary of crystallographic data (Table S3).

Acknowledgments

This work was financially supported by the Grant Agency of Charles University in Prague (grant number 69309) and by the Ministry of Education, Youth and Sports of the Czech Republic (project number MSM0021620857).

[1] P. Štěpnička, *Chem. Soc. Rev.* **2012**, *41*, 4273–4305.
[2] a) *Aqueous-Phase Organometallic Chemistry* (Eds.: B. Cornils, W. A. Herrmann), 2nd ed., Wiley-VCH, Weinheim, Germany, **2004**; b) F. Joó, *Aqueous Organometallic Catalysis*, Kluwer, Dordrecht, The Netherlands, **2001**.

[3] a) *Ferrocenes – Homogeneous Catalysis, Organic Synthesis, Materials Science* (Eds.: A. Togni, T. Hayashi), Wiley-VCH, Weinheim, Germany, **1995**; b) *Ferrocenes – Ligands, Materials and Biomolecules* (Ed.: P. Štěpnička), Wiley, Chichester, UK, **2008**.

[4] For selected reviews, see: a) R. C. J. Atkinson, V. Gibson, N. J. Long, *Chem. Soc. Rev.* **2004**, *33*, 313–328; b) P. Barbaro, C. Bianchini, G. Giambastiani, S. L. Parisel, *Coord. Chem. Rev.* **2004**, *248*, 2131–2150; c) R. Goméz Arrayás, J. Adrio, J. C. Carretero, *Angew. Chem.* **2006**, *118*, 7836; *Angew. Chem. Int. Ed.* **2006**, *45*, 7674–7715.

[5] a) X. Feng, B. Pugin, E. Küsters, G. Sedelmeier, H.-U. Blaser, *Adv. Synth. Catal.* **2007**, *349*, 1803–1807; b) B. Pugin, Patent WO 2001004131 A1 (**2001**).

[6] a) J. Podlaha, P. Štěpnička, J. Ludvík, I. Císařová, *Organometallics* **1996**, *15*, 543–550; b) P. Štěpnička, *Eur. J. Inorg. Chem.* **2005**, 3787–3808.

[7] J. Schulz, I. Císařová, P. Štěpnička, *Organometallics* **2012**, *31*, 729–738.

[8] a) J. Tauchman, I. Císařová, P. Štepnička, *Organometallics* **2009**, *28*, 3288–3302; b) J. Tauchman, I. Císařová, P. Štěpnička, *Eur. J. Org. Chem.* **2010**, 4276–4287; c) J. Tauchman, I. Císařová, P. Štěpnička, *Dalton Trans.* **2011**, *40*, 11748–11757; d) J. Tauchman, B. Therrien, G. Süss-Fink, P. Štěpnička, *Organometallics* **2012**, *31*, 3985–3994.

[9] a) J. Schulz, I. Císařová, P. Štěpnička, *J. Organomet. Chem.* **2009**, *694*, 2519–2530; b) J. Schulz, A. K. Renfrew, I. Císařová, P. J. Dyson, P. Štěpnička, *Appl. Organomet. Chem.* **2010**, *24*, 392–397.

[10] A prominent but rather solitary example of phosphanyl carboxamides with 2-hydroxyethyl groups is undoubtedly 2-(diphenylphosphanyl)-*N*-(2-hydroxyethyl)benzamide, which was studied as a ligand in Re^{V} complexes and because of its prospective applications in nuclear medicine: a) J. D. G. Correia, Â. Domingos, A. Paulo, I. Santos, *J. Chem. Soc., Dalton Trans.* **2000**, 2477–2482; b) J. D. G. Correia, Â. Domingos, I. Santos, *Eur. J. Inorg. Chem.* **2000**, 1523–1529; c) J. D. G. Correia, Â. Domingos, I. Santos, H. Spies, *J. Chem. Soc., Dalton Trans.* **2001**, 2245–2250; d) J. D. G. Correia, Â. Domingos, I. Santos, R. Alberto, K. Ortner, *Inorg. Chem.* **2001**, *40*, 5147–5151; e) T. Kniess, J. D. G. Correia, Â. Domingos, E. Palma, I. Santos, *Inorg. Chem.* **2003**, *42*, 6130–6135; f) C. Fernandes, J. D. G. Correia, L. Gano, I. Santos, S. Seifert, R. Syhre, R. Bergmann, H. Spies, *Bioconjugate Chem.* **2005**, *16*, 660–668.

[11] To the best of our knowledge, there is no report concerning the preparation of phosphanylamides from $H_2NCH(CH_2OH)_2$ (serinol).

[12] a) 3-(Diphenylphosphanyl)-*N*-[2-hydroxy-1,1-bis(hydroxymethyl)ethyl]propanamide, a hydrophilic phosphane prepared by the addition of diphenylphosphane to CH_2=CHCONHC-$(CH_2OH)_3$, was studied as a ligand for Rh comlexes: L. Lavenot, M. H. Bortoletto, A. Roucoux, C. Larpent, H. Patin, *J. Organomet. Chem.* **1996**, *509*, 9–14; b) Amides of the type $RC(O)NHCH_2\{CH_2O(CH_2)_3NHC(O)CH_2P(O)Y_2\}_3$, where Y = R′ or OR′, and some related compounds were evaluated in extractions of metal ions: M. M. Reinoso-García, D. Janczewski, D. N. Reinhoudt, W. Verboom, E. Malinowska, M. Pietrzak, C. Hill, J. Báča, B. Grüner, P. Selucky, C. Grüttner, *New J. Chem.* **2006**, *30*, 1480–1492.

[13] For related phosphanylferrocenecarboxamides, see: a) W. Zhang, T. Shimanuki, T. Kida, Y. Nakatsuji, I. Ikeda, *J. Org. Chem.* **1999**, *64*, 6247–6251; b) M. Lamač, I. Císařová, P. Štěpnička, *New J. Chem.* **2009**, *33*, 1549–1562.

[14] a) A. El-Faham, F. Albericio, *Chem. Rev.* **2011**, *111*, 6557–6602 (review article) b) B. Belleau, G. Malek, *J. Am. Chem. Soc.* **1968**, *90*, 1651–1652.

[15] For an example of the application of EEDQ in the synthesis of amides from $HOC(CH_2OH)_3$, see: I. Villanueva, B. Hernandez, V. Chang, M. D. Heagy, *Synthesis* **2000**, 1435–1438.

[16] W. Zhang, Y. Yoneda, T. Kida, Y. Nakatsuji, I. Ikeda, *Tetrahedron: Asymmetry* **1998**, *9*, 3371–3380.

[17] a) H. Jendralla, E. Paulus, *Synlett* **1997**, 471–472; b) J. Kühnert, M. Dušek, J. Demel, H. Lang, P. Štěpnička, *Dalton Trans.* **2007**, 2802–2811; c) J. Kühnert, I. Císařová, M. Lamač, P. Štěpnička, *Dalton Trans.* **2008**, 2454–2464; d) P. Štěpnička, H. Solařová, M. Lamač, I. Císařová, *J. Organomet. Chem.* **2010**, *695*, 2423–2431; e) P. Štěpnička, H. Solařová, I. Císařová, *J. Organomet. Chem.* **2011**, *696*, 3727–3740.

[18] a) T. Gramstad, *Acta Chim. Scand.* **1961**, *15*, 1337–1346; b) J. Mendel, A. Kolbe, *Phosphorus Sulfur Relat. Elem.* **1977**, *3*, 21–26; c) E. V. Ryl′tsev, A. K. Shurubura, Y. P. Egorov, V. Y. Semenii, *Teoret. Eksperiment. Khim.* **1980**, *16*, 497–503; d) For a report concerning ferrocenylphosphanes and the corresponding phosphane oxides, see: L. M. Ephstein, E. S. Shubina, A. I. Krylova, V. S. Tolkunova, V. D. Vil'chevskaya, D. N. Kravtsov, *Izv. Akad. Nauk SSR, Ser. Khim.* **1987**, 572–575.

[19] a) P. Štěpnička, I. Císařová, *New J. Chem.* **2002**, *26*, 1389–1396; b) B. F. M. Kimmich, C. R. Landis, D. R. Powell, *Organometallics* **1996**, *15*, 4141–4146.

[20] A search for intermolecular P···H–O contacts in the Cambridge Crystallographic Database (version 5.33 of November 2011 and updates of November 2011, February 2012, and May 2012) yielded eleven results (refcodes: BAXPUM, FEQKOC, GOSLUV, KUYBOW, LAGMIR, MULXIA, NAPYIM, OKAZIJ, TOCHIC, TOCHOI, and TOXGAO). The shortest (strongest) contacts were detected for phosphanylphenols having acidic OH groups (P···O ca. 3.2–3.5 Å). For references, see: a) J. Heinicke, R. Kadyrov, M. K. Kindermann, M. Koesling, P. G. Jones, *Chem. Ber.* **1996**, *129*, 1547–1560; b) R. Kadyrov, J. Heinicke, M. K. Kindermann, D. Heller, C. Fischer, R. Selke, A. K. Fischer, P. G. Jones, *Chem. Ber./Recueil* **1997**, *130*, 1663–1670; c) P. Schober, G. Huttner, A. Jacobi, *J. Organomet. Chem.* **1998**, *571*, 279–288.

[21] The sum of the N–H···O and O···H···O angles around H1N is 346°.

[22] π–π-Stacking interactions were detected for phenyl ring C(12–17) and its inverted (parallel) image, and the distance between the respective ring centroids is 4.140(2) Å.

[23] A search for P=O···O–H contacts in the Cambridge Crystallographic Database (version as above) yielded 203 results with $R < 10\%$ and free of a disorder. Histograms showing the distribution of the O···O distances and the O–H···O angles (see Supporting Information, Figures S3 and S4) clearly indicate the directional nature of these interactions.

[24] The complexes often give rise to very broad and sometimes multiple $^{31}P\{^{1}H\}$ NMR resonances, which is due to slow structural dynamics. Upon increasing the temperature of the measurement, the signals become sharper and collapse into singlet resonances.

[25] P. Štěpnička, J. Demel, J. Čejka, *J. Mol. Catal. A* **2004**, *224*, 161–169.

[26] For **5c**·CH_2Cl_2: Cg3–Ru–Cl1 125.83(4)°, Cg3–Ru–Cl2 123.22(4)°, Cg3–Ru–P 134.00(4)°; for **6c**·Et_2O_2: Cg3–Ru–Cl1 126.27(4)°, Cg3–Ru–Cl2 123.27(4)°, Cg3–Ru–P 134.90(4)°; Cg3 denotes the centroid of the η^6-benzene ring.

[27] The dihedral angles subtended by these planes are 20.8(1)° and 19.9(1)° for **5c**·CH_2Cl_2 and **6c**·Et_2O, respectively.

[28] a) R. C. van der Drift, E. Bouwman, E. Drent, *J. Organomet. Chem.* **2002**, *650*, 1–24; b) R. Uma, C. Crévisy, R. Grée, *Chem. Rev.* **2003**, *103*, 27–51.

[29] For recent reviews, see: a) V. Cadierno, P. Crochet, J. Gimeno, *Synlett* **2008**, 1105–1124; b) N. Ahlsten, A. Bartoszewicz, B. Martín-Matute, *Dalton Trans.* **2012**, *41*, 1660–1670; c) P. Lorenzo-Luis, A. Romerosa, M. Serrano-Ruiz, *ACS Catal.* **2012**, *2*, 1079–1086.

[30] a) C. Slugovc, E. Rüba, R. Schmid, K. Kirchner, *Organometallics* **1999**, *18*, 4230–4233; b) I. E. Markó, A. Gautier, M. Tsukazaki, A. Llobet, E. Plantalech-Mir, C. J. Urch, S. M. Brown, *Angew. Chem.* **1999**, *111*, 2126; *Angew. Chem. Int. Ed.* **1999**,

38, 1960–1962; c) C. Bianchini, A. Meli, W. Oberhauser, *New J. Chem.* **2001**, *25*, 11–12; d) R. C. van der Drift, J. W. Sprengers, E. Bouwman, W. P. Mul, H. Kooijman, A. L. Spek, E. Drent, *Eur. J. Inorg. Chem.* **2002**, 2147–2155; e) B. Martín-Matute, K. Bogár, M. Edin, F. B. Kaynak, J.-E. Bäckvall, *Chem. Eur. J.* **2005**, *11*, 5832–5842; f) P. Crochet, M. A. Fernández-Zúmel, J. Gimeno, M. Scheele, *Organometallics* **2006**, *25*, 4846–4849; g) N. Ahlsten, H. Lundberg, B. Martín-Matute, *Green Chem.* **2010**, *12*, 1628–1633; h) M. Batuecas, M. A. Esteruelas, C. García-Yebra, E. Oñate, *Organometallics* **2010**, *29*, 2166–2175; i) A. P. da Costa, J. A. Mata, B. Royo, E. Peris, *Organometallics* **2010**, *29*, 1832–1838; j) V. Bizet, X. Pannecoucke, J.-L. Renaud, D. Cahard, *Angew. Chem. Int. Ed.* **2012**, *51*, 6467–6470.

[31] For a review on asymmetric isomerizations of allylic alcohols, see: L. Mantilli, C. Mazet, *Chem. Lett.* **2011**, *40*, 341–344.

[32] K. Tanaka, G. C. Fu, *J. Org. Chem.* **2001**, *66*, 8177–8186.

[33] Selected reviews: a) S. Ribe, P. Wipf, *Chem. Commun.* **2001**, 299–307; b) J. B. F. N. Engberts, M. J. Blandamer, *Chem. Commun.* **2001**, 1701–1708; c) C. J. Li, *Chem. Rev.* **2005**, *105*, 3095–3165; d) M. C. Pirrung, *Chem. Eur. J.* **2006**, *12*, 1312–1317; e) R. N. Butler, A. G. Coyne, *Chem. Rev.* **2010**, *110*, 6302–6337; f) M. O. Simon, C.-J. Li, *Chem. Soc. Rev.* **2012**, *41*, 1415–1427.

[34] a) V. Cadierno, S. E. García-Garrido, J. Gimeno, *Chem. Commun.* **2004**, 232–233; b) V. Cadierno, S. E. García-Garrido, J. Gimeno, A. Varela-Álvarez, J. A. Sordo, *J. Am. Chem. Soc.* **2006**, *128*, 1360–1370; c) T. Campos-Malpartida, M. Fekete, F. Joó, Á. Kathó, A. Romerosa, M. Saoud, W. Wojtków, *J. Organomet. Chem.* **2008**, *693*, 468–474; d) P. Servin, R. Laurent, L. Gonsalvi, M. Tristany, M. Peruzzini, J.-P. Majoral, A.-M. Caminade, *Dalton Trans.* **2009**, 4432–4434; e) J. García-Álvarez, J. Gimeno, F. J. Suárez, *Organometallics* **2011**, *30*, 2893–2896; f) L. Bellarosa, J. Díez, J. Gimeno, A. Lledós, F. J. Suárez, G. Ujaque, C. Vicent, *Chem. Eur. J.* **2012**, *18*, 7749–7765.

[35] a) V. Cadierno, P. Crochet, S. E. García-Garrido, J. Gimeno, *Dalton Trans.* **2004**, 3635–3641; b) P. Crochet, J. Díez, M. A. Fernández-Zúmel, J. Gimeno, *Adv. Synth. Catal.* **2006**, *348*, 93–100; c) A. E. Díaz-Álvarez, P. Crochet, M. Zablocka, C. Duhayon, V. Cadierno, J. Gimeno, J.-P. Majoral, *Adv. Synth. Catal.* **2006**, *348*, 1671–1679; d) M. Fekete, F. Joó, *Catal. Commun.* **2006**, *7*, 783–786; e) B. Lastra-Barreira, J. Díez, P. Crochet, *Green Chem.* **2009**, *11*, 1681–1686; f) A. Azua, S. Sanz, E. Peris, *Organometallics* **2010**, *29*, 3661–3664.

[36] A. Chanda, V. V. Fokin, *Chem. Rev.* **2009**, *109*, 725–74.

[37] R. A. Zelonka, M. C. Baird, *Can. J. Chem.* **1972**, *50*, 3063–3072.

[38] M. A. Bennett, T.-N. Huang, T. W. Matheson, A. K. Smith, *Inorg. Synth.* **1982**, *21*, 74–78.

[39] X. Wang, R. Liu, Y. Jin, X. Liang, *Chem. Eur. J.* **2008**, *14*, 2679–2685.

[40] D. J. Fox, D. S. Pedersen, S. Warren, *Org. Biomol. Chem.* **2006**, *4*, 3102–3107.

[41] S. Pääkkönen, J. Pursiainen, M. Lajunen, *Tetrahedron Lett.* **2010**, *51*, 6695–6699.

[42] M. Puchberger, W. Rupp, U. Bauer, U. Schubert, *New J. Chem.* **2004**, *28*, 1289–1294.

[43] S. A. Van Arman, *Tetrahedron Lett.* **2009**, *50*, 4693–4695.

[44] M. R. Rohman, M. Rajbangshi, B. M. Laloo, P. R. Sahu, B. Myrboh, *Tetrahedron Lett.* **2010**, *51*, 2862–2864.

[45] R. J. Abraham, M. Mobli, J. Ratti, F. Sancassan, T. A. D. Smith, *J. Phys. Org. Chem.* **2006**, *19*, 384–392.

[46] Z. Otwinowski, W. Minor, *Methods Enzymol.* **1997**, *276*, 307–326.

[47] A. Altomare, M. C. Burla, M. Camalli, G. L. Cascarano, C. Giacovazzo, A. Guagliardi, A. G. G. Moliterni, G. Polidori, R. Spagna, *J. Appl. Crystallogr.* **1999**, *32*, 115–119.

[48] G. M. Sheldrick, *Acta Crystallogr., Sect. A* **2008**, *64*, 112–122.

[49] P. van der Sluis, A. L. Spek, *Acta Crystallogr., Sect. A* **1990**, *46*, 194–201.

[50] A. L. Spek, *J. Appl. Crystallogr.* **2003**, *36*, 7–13.

Received: July 2, 2012
Published Online: ■

Polar Phosphanyl Carboxamides

Ruthenium(II) complexes of the type [(η^6-arene)$RuCl_2$(L)], obtained from phosphanylferrocenecarboxamides bearing polar hydroxyalkyl pendants and the respective dimers [(η^6-arene)$RuCl_2]_2$ (arene = C_6H_6, *p*-cymene, C_6Me_6), were evaluated as catalysts for redox isomerizations of allylic alcohols to the corresponding carbonyl compounds.

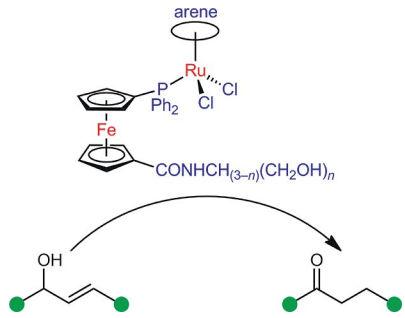

Keywords: Metallocenes / Structure elucidation / Isomerization / Phosphane ligands / Ruthenium

